Cell Reports, Volume *30*

Supplemental Information

The Cap-Snatching SFTSV Endonuclease Domain Is an Antiviral Target

Wenjie Wang, Woo-Jin Shin, Bojie Zhang, Younho Choi, Ji-Seung Yoo, Maxwell I. Zimmerman, Thomas E. Frederick, Gregory R. Bowman, Michael L. Gross, Daisy W. Leung, Jae U. Jung, and Gaya K. Amarasinghe

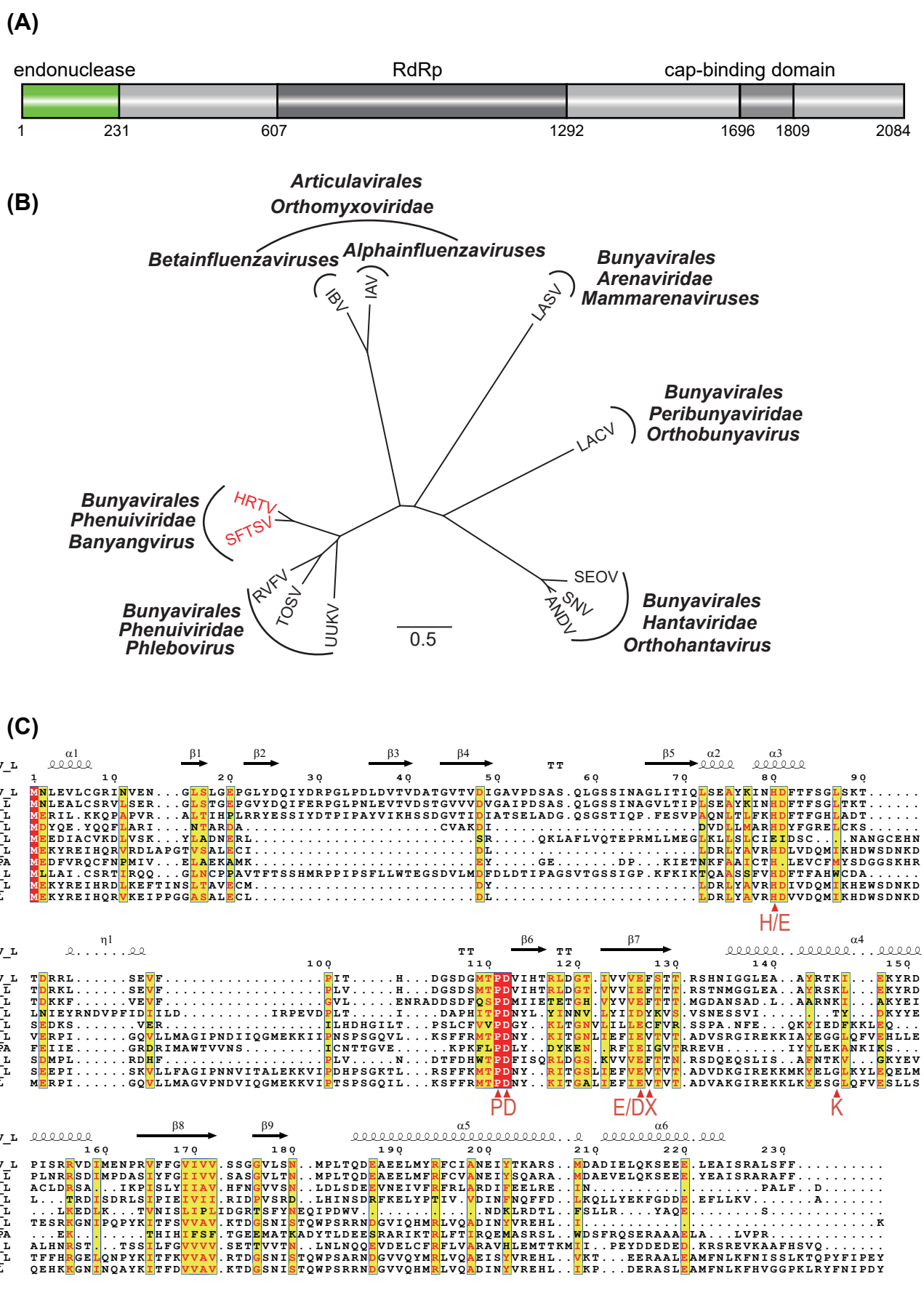

Figure S1. Sequence analysis of SFTSV and bunyaviruses. Related to Fig 1 and 2. (A) Domain organization of SFTSV L protein sequence used in the current study. **(B)** A phylogenic tree of bunyaviruses and arthomyxociruses was performed by aligning the full L protein sequence using Geneious Prime software (Geneious Prime 2019.2). **(C)** Structure-based sequence alignment of endonuclease domains show high sequence conservation. Details in the STAR Methods.

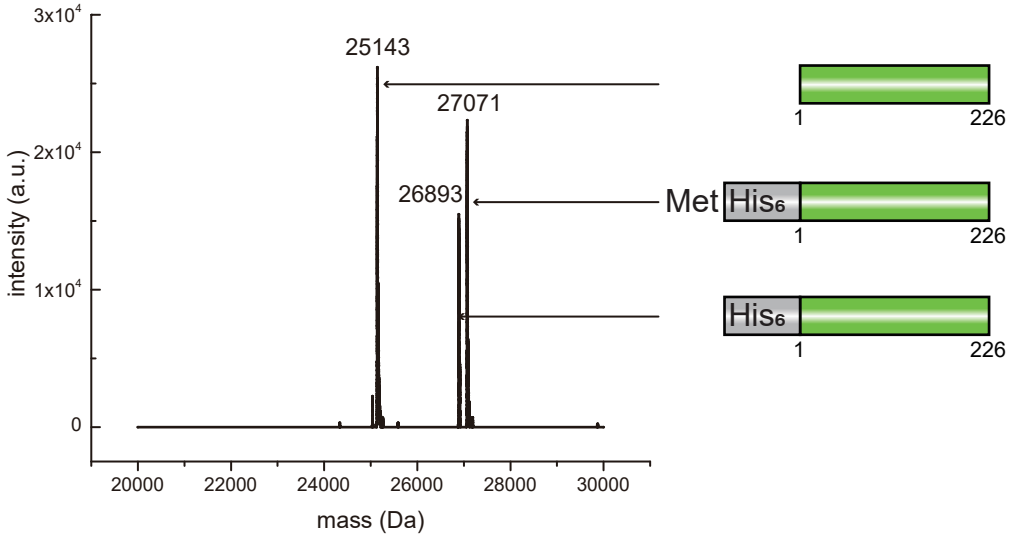

Figure S2. Native mass spectrometry anaysis. Related to Fig 1. Intact mass measurement of a SFTSV L 1-231 aa crystal using LC/MS. Deconvoluted mass spectrum of SFTSV L 1-231 aa during cystalization screening (no Se-Met). Determined mass of the crystal by LC-MS was 25143 Da. The theoretical mass for SFTSV L 1-226 aa is 25143 Da, suggesting that the Met-His_6-tag and SFTSV L residues 227-231 were cleaved by trypsin. The 26893 Da species is the His_6-tagged SFTSV L 1-226 aa with methionine cleaved. The 27071 Da is Met-His_6-tagged SFTSV L 1-226 aa with a +46 Da modification on the first methionine.

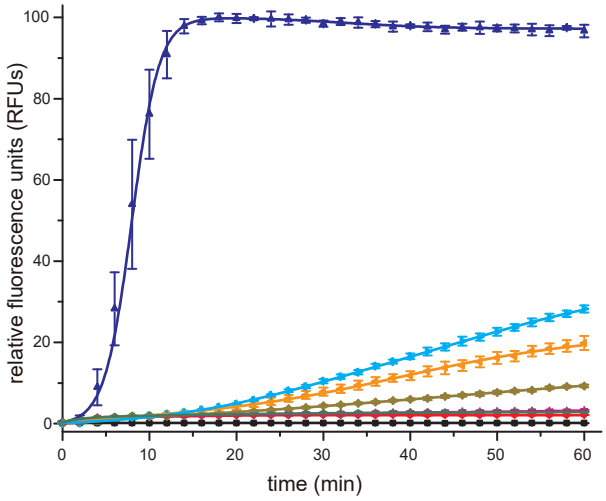

Figure S3. FRET-based endonuclease assay curves with different ions. Related to Fig 3. FRET-based experiments are shown for endonuclease reactions of SFTSV L 1-231 aa with 1 mM $MnCl_2$ (blue), 1 mM $MgCl_2$ (magenta), 5 mM $MgCl_2$ (dark yellow), 10 mM $MgCl_2$ (orange), 20 mM $MgCl_2$ (cyan), 1 mM $CaCl_2$ (olive) and no ions (red). Buffer only (black) was included as a control. Experiments were carried out in triplicate and average data are shown with error bars representing the standard deviation.

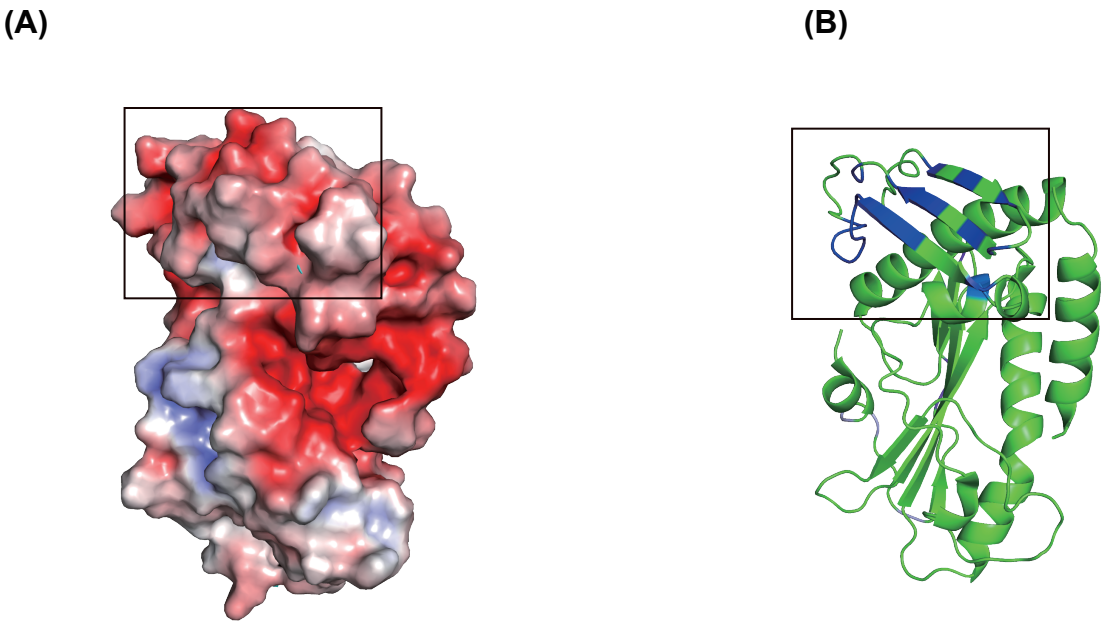

Figure S4. The surface β-sheet region is predicted to be associated with protein-protein interactions. Related to Fig 2. **(A**) Electrostatic representation of the SFTSV endonuclease domain. **(B)** Residues (colored in blue) within the surface β-sheet region are predicted to be associated with protein-protein interactions. The surface β-sheet region is outlined with the box.

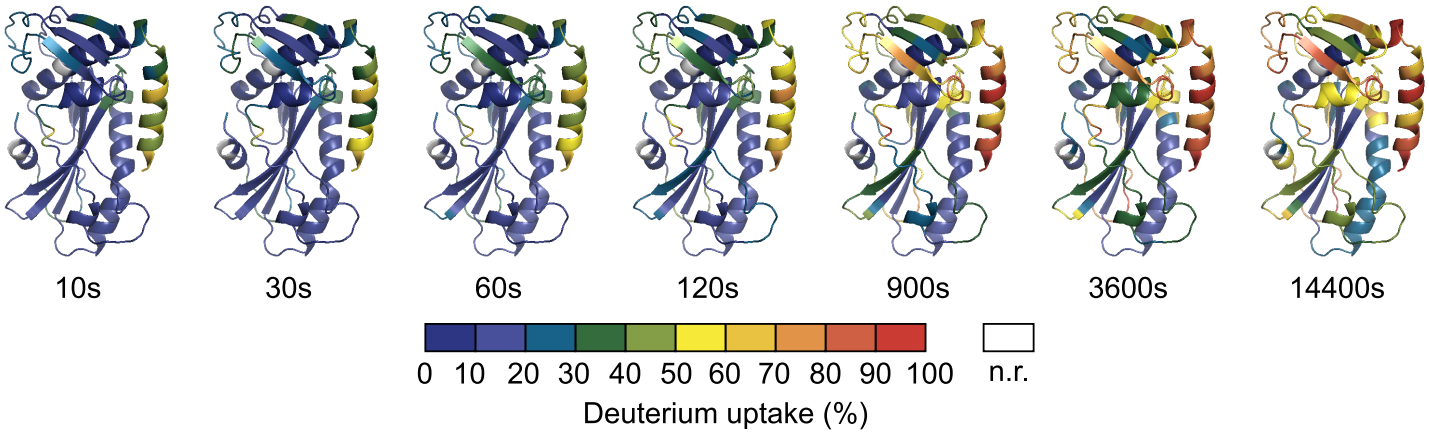

Figure S5. HDX -MS heat map of SFTSV L 1-231 aa. Related to Fig 4C. HDX -MS results mapped on the cartoon representation of SFTSV L 1-231 aa crystal structure. The percentages of deuterium incorporation from different D_2O-incubation times (10 s, 30 s, 60 s, 120 s, 900 s, 3,600 s and 14,400 s) are mapped using color
gradient shown below, where cooler colors represent regions with lower percentages of deuterium uptake and warmer colors represent regions with higher percentages of deuterium uptake. Data shown are the average of duplicate samples.

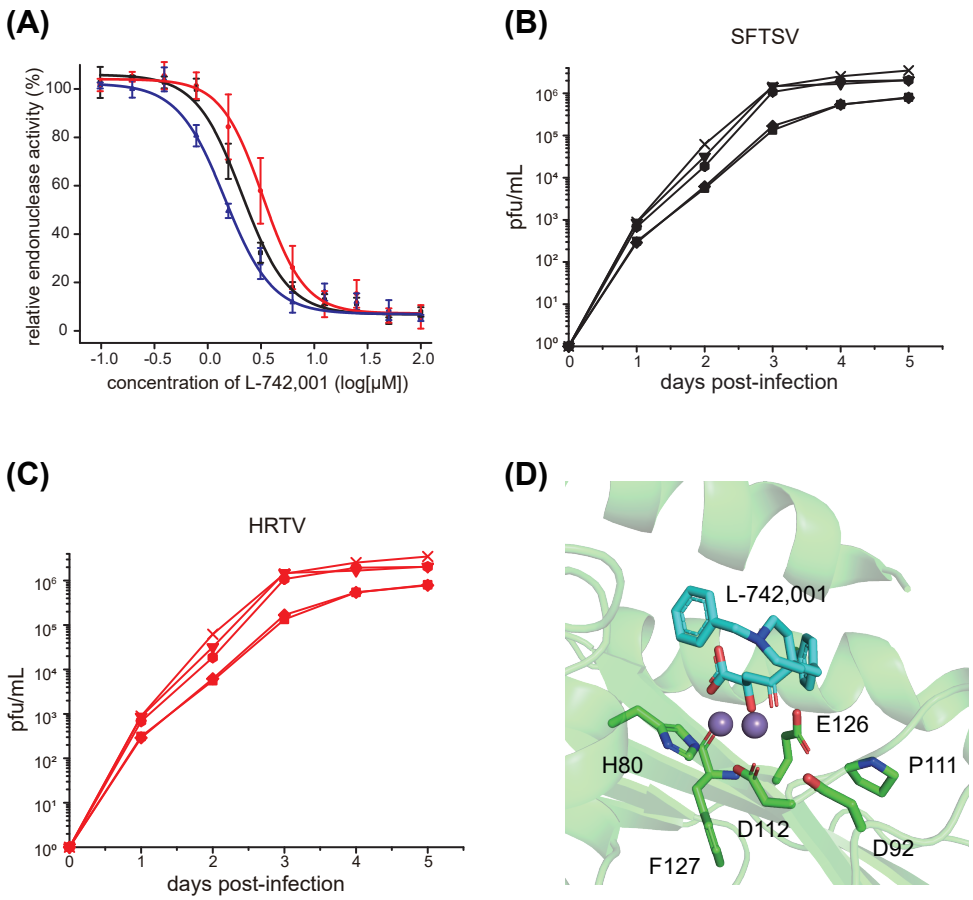

Figure S6. Enzyme inhibition assay and Virus growth inhibition assay of SFTSV, HRTV and Influenza virus. Related to Fig 5. (A) Endonuclease inhibition was measured for SFTSV L 1-231 aa (black), HRTV L 1-231 aa (red), or IAV PA 1-192 aa (blue) in presence of difference concentrations of L-742,001. Fluorescence values were expressed as percentages of non-treated controls, and EC_{50} (50% effective concentration) values of the test compound were determined. Cell cultures were used to determine the virus growth properties. **(B)** SFTSV or **(C)** HRTV was infected at a MOI of 0.01 in Vero E6 cells with different concentrations of L-742,001 (100 μM, black; 50 μM, red; 25 μM, blue; 12.5 μM, orange; 0 μM, cyan) in quintuplicate. Cultures were collected every 24 hrs and subjected to plaque assay. **(D)** Docking simulation of two Manganese ions (purple) and L-742,001 (cyan) with SFTSV L 1-231 aa (green).

Table S1. RMSD pairwise values, and number of equivalent positions in parenthesis, calculated from pairwise structural alignments using Superpose with the endonucleases used in this study: TOSV (6QW5), LACV (2XI5), LASV (5J1P), ANDV (5HSB) and Influenza A virus (5DES) and SFTSV L endonuclease structures. The molecule in the asymmetric unit used in the alignment is indicated in parenthesis for each PDB. Related to Fig 2.

	TOSV(A)	LACV(A)	LASV(A)	ANDV(A)	IAV(A)
SFTSV(A)	1.93 Å (177 residues)	3.12 Å (94 residues)	2.87 Å (107 residues)	2.84 Å (117 residues)	3.46 Å (102 residues)

Table S2. IC_{50} values of endonuclease inhibitors tested. Related to Fig 5A and S6A

	IC_{50} (μM)	
	L-742,001	BXA
SFTSV L 1-231 aa	2.1 ± 0.2	0.14 ± 0.005
HRTV L 1-231 aa	3.3 ± 0.4	0.12 ± 0.002
IAV PA 1-192 aa	1.4 ± 0.1	0.036 ± 0.003

Table S3. Data collection and refinement statistics. Related to Fig 1.

	Se-Met SFTSV L 1-231	Se-Met SFTSV L 1-231
Data collection		
Wavelength	0.9792	0.9792
Resolution range	46.63-2.50 (2.59-2.50)	47.09 - 2.40 (2.49 - 2.40)
Space group	$P4_32_12$	$P4_32_12$
Unit cell		
a, b, c (Å)	83.0 83.0 230.2	82.7 82.7 229.1
α, β, γ (°)	90 90 90	90 90 90
Total reflections	366112 (36068)	247530 (24903)
Unique reflections	53114 (4471)	32031 (2936)
Multiplicity	6.9 (6.8)	7.7 (8.0)
Completeness (%)	97.91 (84.36)	98.90 (93.83)
Mean I/sigma(I)	10.86 (2.72)	14.02 (4.10)
Wilson B-factor	35.72	36.39
R-merge	0.2193 (1.527)	0.1225 (0.7682)
R-meas	0.2373 (1.655)	0.1316 (0.8235)
R-pim	0.09017 (0.6331)	0.04736 (0.2938)
CC1/2	0.991 (0.520)	0.997 (0.798)
CC*	0.998 (0.827)	0.999 (0.942)
Phase determination, structure solution, and refinement		
Anomalous scatterer	Selenium (18 sites)	
Figure of merit	0.306	
Reflections used in refinement	52027 (4471)	31736 (2936)
Reflections used for R-free	2488 (220)	2000 (185)
R-work	0.3025 (0.3400)	0.2005 (0.2448)
R-free	0.3653 (0.4006)	0.2380 (0.2857)
CC(work)		0.955 (0.845)
CC(free)		0.927 (0.815)
Number of non-hydrogen atoms		5419
macromolecules		5229
solvent		190
Protein residues		678
RMS(bonds)		0.006

RMS(angles)	1.21
Ramachandran favored (%)	97.92
Ramachandran allowed (%)	2.08
Ramachandran outliers (%)	0.00
Rotamer outliers (%)	0.00
Clashscore	6.27
MolProbity Score	1.36
Average B-factor	42.30
macromolecules	42.39
solvent	39.75
PDB ID	6NTV